PUNCH-THROUGH IN THE NORTH SEA: A COMPARISON AMONG DIFFERENT ANALYSIS METHODS

J. Gallacchi* and S. Raymackers
Engineering Department, DEME Offshore
DEME Group, Belgium

** corresponding author: gallacchi.julien@deme-group.com*

ABSTRACT
This paper aims at comparing different calculation methods used to calculate bearing capacity of sand layers overlying clay, starting from CPT data and by using leg penetrations records from completed projects in the North Sea, where the stratigraphy is known, and tertiary soil layers show limited variation in their strength. Furthermore, locations with thick soil layers were selected, to minimize the influence of different shear strengths in consecutive clay layers. Parameters such as N_{kt} values are first validated in locations where the final spudcan penetration was located within a clay layer. Then, predictions on leg penetrations are performed starting with different methods for estimating the bearing capacity of sand overlying clay. These are finally compared with the recorded penetrations, providing a performance overview of each method.

KEY WORDS: *Punch-through, North Sea, Load-spread method, Hanna & Meyerhof method, Hu method*

1 INTRODUCTION
In recent years, the North Sea has seen a sharp increase of offshore wind capacity, as its favourable conditions facilitate the construction of wind farms. DEME Offshore, DEME's activity line specialized in offshore marine engineering projects (previously GeoSea), has been playing a leading role in multiple design and construction projects in the North Sea and it disposes of a vast database, ranging from offshore geophysical and geotechnical measurements collected during site investigations to operational logs recorded during a project's execution. A fundamental step for the execution of such projects is the Leg Penetration Assessment (LPA). One key challenge of these analyses is to correctly predict the occurrences of a punch-through, which typically (but not exclusively) occurs when a dense sand is overlying a weaker clay layer.

The focus of this paper is to compare three different methods of estimating the bearing capacity of sand overlying a weak clay layer. Namely, the method of Hanna & Meyerhof (1980), the load-spread method (ISO 19905-1, 2016), and the method proposed by Hu et al. (2014). The data from two completed projects in the North Sea (Project A and Project B), sharing the same soil units and a similar stratigraphy, are considered. Locations with a superficial sand layer (Quaternary Sand) overlying a tertiary clay layer (Ursel Clay) were selected. The soil profiles at these locations were characterised using the corresponding CPT data. In the first part of this paper, the groundwork for the analyses is presented. The second part focuses on the calibration of the cone factor N_{kt}, which provides a linear relation between CPT data and the undrained shear strength of clays, and a summary of the considered soil profiles is provided The third part briefly introduces the different methods considered for predicting the soil resistance of a two-layer system. The fourth part presents the prediction results obtained with the different methods and compares them with the recorded leg penetrations. Finally, the results are discussed in the conclusion paragraph.

2 LEG PENETRATION ASSESSMENT
A leg penetration assessment is performed by combining the leg and / or spudcan specifications with the available geotechnical data.

2.1 SPUDCAN SPECIFICATIONS
Three different jack-up vessels (V1, V2 and V3) were considered in this paper, of which one was used at both projects. All three vessels have truss legs with spudcans at their tips. The vessel data used in the calculations are listed in Table 1.

Table 1: Relevant vessel data for LPA analyses.

Vessel	Project	Locations	B [m]	A [m^2]	V_{spud} [m^3]	V_D [m^3]	Preload pressure range [kPa]	Tip correction [m]
V1	A, B	9 + 19	17.4	240	410	45.35	532.4 – 607.6	0
V2	A	9	15.5	190	0	0	330.4 – 371.2	1.5
V3	B	10	13.4	140	0	0	434.0 – 451.0	1.5

All spudcans were modelled as flat circular footings in all 3 methods, thus considering an equivalent spudcan diameter (V2 and V3 have rectangular and square spudcans, respectively). Because of the large impact, for the Hu et al. method both cases (flat footing and conical footing) were considered.
The tip correction is used to reduce the recorded penetration data, since the reported values are the depth of the spudcan tip, but predictions are made at the depth of B.

2.2 LEG PENETRATION BEHAVIOUR

For all locations the final leg penetrations are measured, for some also the complete preloading was monitored.
An example of the load penetration behaviour for Vessel 1 at Location A3 is given in Figure 1. It can be seen how the technique of overshooting (Versteele, Cathie, Kuo, & Raymackers, 2017) is applied in this case.

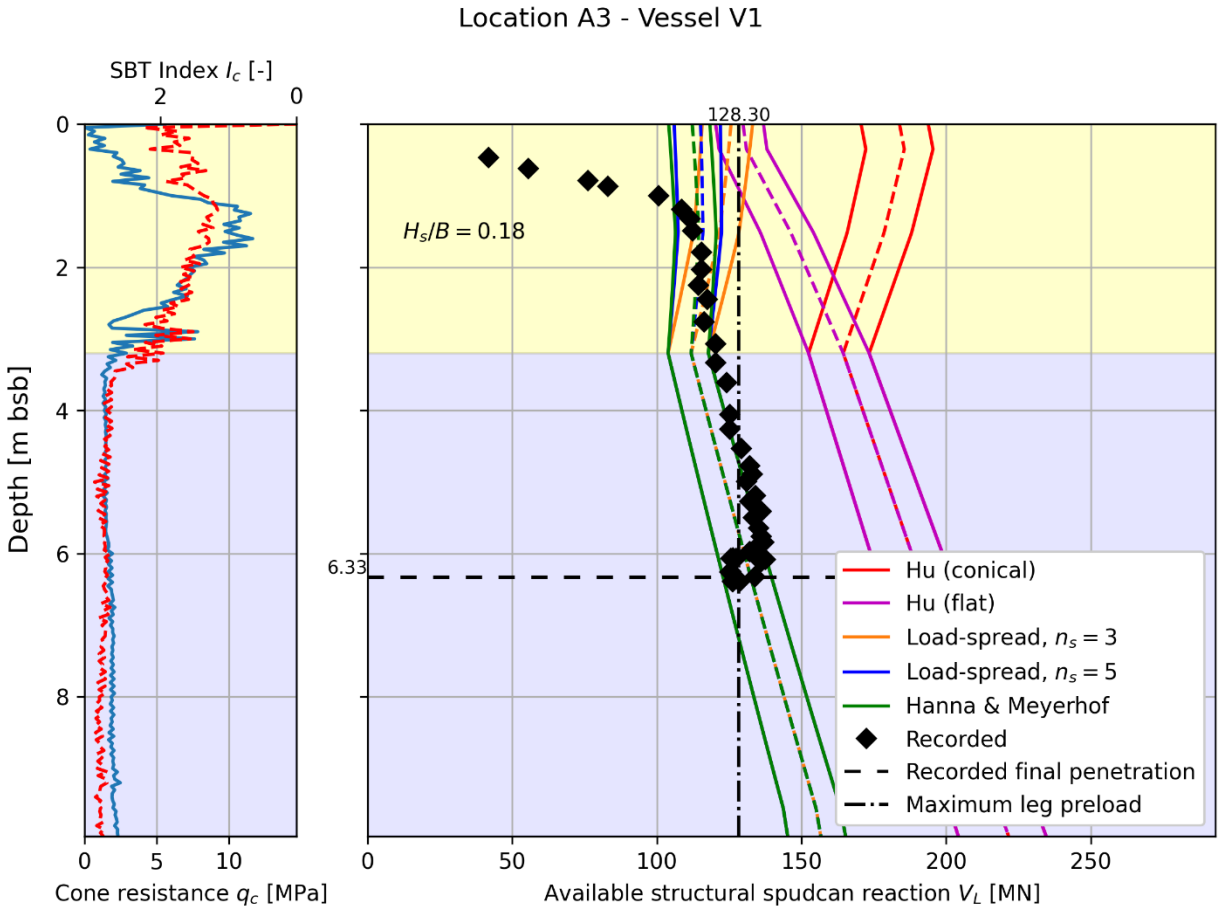

Figure 1: Left: CPT profile (blue full line) and Ic (red dashed line). Right: predicted leg penetrations with different methods together with recorded load-penetration behaviour of Vessel 1 at Location A3.

2.3 LOCATIONS

Nine locations visited by two distinct vessels (Vessel V1 and Vessel V2) were considered from Project A. From Project B, 19 locations were considered, all of which were visited by Vessel 1, and ten by Vessel V3.

All locations have a surficial layer of Quaternary Sand of variable thickness, lying over a layer of Ursel Clay. The sites have been chosen because the stratigraphy is well documented (Le Bot, Van Lancker, Deleu, De Batist, & Henriet, 2003), and the soil layers have been well characterised throughout the windfarm area's. Note that only the logs of the jack-up leg closest to the CPT location were considered, to minimize the effects of soil variability.

Table 2: Analysed locations.

Project Location	Visiting vessels	Preload pressure [kPa]	Sand layer thickness [m]	Clay layer thickness [m]	Recorded penetration [m]	Corrected recorded penetration [m]	Occurrence of punch-through
A1	V1 / V2	561.05 / 350.48	0.4	13.6	6.15 / 4.00	6.15 / 2.50	Yes / Yes
A2	V1 / V2	561.46 / 343.30	1.8	11.8	7.36 / 3.10	7.36 / 1.60	Yes / Yes
A3	V1 / V2	534.56 / 346.96	3.2	14.9	6.33 / 3.20	6.33 / 1.70	Yes / No
A4	V1 / V2	545.64 / 345/05	5.3	13.6	4.68 / 1.20	4.68 / 0.00	Yes / No
A5	V1 / V2	570.49 / 371.23	4.9	13.4	0.75 / 1.00	0.75 / 0.00	No / No
A6	V1 / V2	564.73 / 351.66	4.9	15.1	0.66 / 0.40	0.66 / 0.00	No / No
A7	V1 / V2	556.84 / 364.52	5.7	16.0	0.92 / 1.20	0.92 / 0.00	No / No
A8	V1 / V2	601.80 / 330.39	2.3	17.7	7.82 / 1.90	7.82 / 0.40	Yes / No
A9	V1 / V2	545.07 / 350.73	3	17.5	6.25 / 1.60	6.25 / 0.10	Yes / No
B1	V1	596.86	7.9	23.4	0.26	0.26	No
B2	V1	555.33	7.3	20.2	0.37	0.37	No
B3	V1 / V3	597.67 / 434.44	8.9	15.6	0.73 / 0.98	0.73 / 0.00	No / No
B4	V1 / V3	591.71 / 450.98	7.8	14.9	0.75 / 0.94	0.75 / 0.00	No / No
B5	V1 / V3	570.41 / 448.90	5	20.9	0.83 / 1.11	0.83 / 0.00	No / No
B6	V1	549.69	4.8	15.5	1.19	1.19	No
B7	V1	594.20	7.7	13.5	0.26	0.26	No
B8	V1	575.48	6.9	16.3	0.7	0.7	No
B9	V1 / V3	587.33 / 435.84	5.8	20.2	0.78 / 1.44	0.78 / 0.00	No / No
B10	V1 / V3	566.57 / 434.02	3.5	16.8	5.5 / 0.96	5.5 / 0.00	Yes / No
B11	V1	576.91	5.5	18.7	0.76	0.76	No
B12	V1	607.61	9	18.3	0.82	0.82	No
B13	V1	595.10	7.5	12.8	0.58	0.58	No
B14	V1	598.33	9.2	6.8	1.09	1.09	No
B15	V1 / V3	532.40 / 435.56	2.3	16.5	4.12 / 1.28	4.12 / 0.00	Yes / No
B16	V1 / V3	538.41 / 435.56	3.5	14.8	4.81 / 3.93	4.81 / 2.43	Yes / No
B17	V1 / V3	576.71 436.76	6.5	3.8	0.99 / 1.61	0.99 / 0.11	No / No
B18	V1 / V3	585.04 / 443.90	6.8	4.3	0.68 / 1.21	0.68 / 0.00	No / No
B19	V1 / V3	577.60 / 439.56	6.9	3.7	1.08 / 1.07	1.08 / 0.00	No / No

For V1 at location A4 and V2 at location A2 it was assumed that punch-through occurred because, even though the spudcan maximum bearing area did not reach the clay layer, the recorded penetration was very close to the sand clay boundary.

2.4 GEOTECHNICAL DATA

At each analysed location, one and up to two CPT data profiles were considered. All relevant geotechnical parameters, namely the Soil Behavior Type Index I_c, the effective friction angle φ' and undrained shear strength s_{u0} were derived directly from CPT data. The N_{kt} values, required to convert cpt cone resistance to undrained shear strength, was further calibrated against the penetration records of locations where the recorded final penetration was located within a clay layer.

2.5 BOTTOM BOUNDARY

The thickness of the Ursel layer is considered sufficient in respect to the penetration depth of the spudcans to omit squeezing effect stemming from the underlying silty clay layer (Asse member).

3 PARAMETER DERIVATION AND SOIL PROFILES

3.1 EFFECTIVE FRICTION ANGLE

The effective friction angle at each location was calculated by first deriving the average relative density of the sand layer using the correlation proposed by Jamiolkowski, Lo Presti, & Manassero (2003), and then relating it to a corresponding friction angle according to Schmertmann (1978), assuming uniform fine sand.

3.2 CONE FACTOR N_{kt}

The cone factor N_{kt} plays a fundamental role in the leg penetration assessment, as it directly relates the corrected cone resistance from CPT records to an undrained shear strength. Site investigations at Project A reported a range of 20 – 30 for the Ursel clay. Site investigations at project B reported a much larger spread, from 6.4 up to 39.8, with a best estimate value of 17.9.

Using the available penetration records, a corresponding N_{kt} could be derived for each location where the spudcan was lying in the Ursel clay. The resulting values are shown in Table 3.

Table 3: Fitted N_{kt} values.

Location	Vessel	N_{kt}
A1	V2	29.67
A1	V1	24.65
A2	V1	26.48
A3	V1	25.25
A8	V1	23.25
A9	V1	24.11
B10	V1	25.51
B15	V1	24.4
B16	V1	24.4

Excluding the case of Vessel V2 at A1, N_{kt} values range from 23.25 to 26.48, providing a good agreement with the value of 26 determined by Sonnema et al. (2023) for Ursel Clay on another site in the Belgian North Sea. All values fall within the ranges reported at Project A and Project B.

Three values were considered for the comparison of the methods, to provide a lower bound (LB), a best estimate (BE) and an upper bound (UB) for the predicted leg penetration: 26.5 for the LB prediction, 24.5 for the BE prediction and 23.3 for the UB prediction. In this phase, the bearing capacity in the clay layer was determined without considering the interaction with the overlying sand layer.

3.3 SOIL PROFILES

The following soil profiles were used for the leg penetration assessment.

Table 4: Soil profiles with summarised parameters.

Project Location	Sand layer thickness [m]	φ' [°]	Clay layer thickness [m]	$s_{um,LB}$ [kPa]	ρ_{LB} [kPa/m]	$s_{um,BE}$ [kPa]	ρ_{BE} [kPa/m]	$s_{um,UB}$ [kPa]	ρ_{UB} [kPa/m]
A1	0.4	33.92	13.6	47.65	3.40	51.44	3.67	54.27	3.87
A2	1.8	34.17	11.8	44.38	4.71	47.91	5.09	50.55	5.37
A3	3.2	36.29	14.9	51.91	3.47	56.04	3.74	59.12	3.95
A4	5.3	37.09	13.6	64.83	3.06	69.99	3.30	73.84	3.48
A5	4.9	39.62	13.4	80.12	1.29	86.49	1.39	91.25	1.47
A6	4.9	38.71	15.1	72.77	2.84	78.55	3.07	82.88	3.24
A7	5.7	37.50	16.0	64.23	2.82	69.33	3.04	73.15	3.21
A8	2.3	34.32	17.7	59.22	2.10	63.93	2.27	67.45	2.39
A9	3	36.42	17.5	59.99	2.08	64.76	2.25	68.32	2.37
B1	7.9	39.93	23.4	90.20	0.32	97.37	0.34	102.73	0.36
B2	7.3	40.88	20.2	91.85	0.00	99.15	0.00	104.61	0.00
B3	8.9	39.06	15.6	84.01	0.98	90.69	1.06	95.68	1.11
B4	7.8	41.45	14.9	80.86	1.54	87.28	1.67	92.09	1.76
B5	5	37.47	20.9	83.21	0.57	89.83	0.62	94.78	0.65
B6	4.8	39.67	15.5	84.34	1.17	91.04	1.26	96.06	1.33
B7	7.7	41.04	13.5	88.35	1.03	95.37	1.12	100.62	1.18
B8	6.9	37.18	16.3	89.29	0.80	96.39	0.87	101.70	0.92
B9	5.8	40.23	20.2	86.57	0.38	93.45	0.41	98.59	0.43
B10	3.5	38.28	16.8	74.10	1.49	79.99	1.61	84.39	1.70
B11	5.5	38.73	18.7	79.91	1.17	86.26	1.26	91.01	1.33
B12	9	39.75	18.3	94.51	0.00	102.02	0.00	107.64	0.00
B13	7.5	39.44	12.8	75.74	2.09	81.76	2.26	86.27	2.38
B14	9.2	38.85	6.8	86.78	4.41	93.68	4.76	98.84	5.03
B15	2.3	36.19	16.5	60.34	2.56	65.13	2.76	68.72	2.91
B16	3.5	35.59	14.8	56.94	3.44	61.46	3.71	64.85	3.92
B17	6.5	40.32	3.8	96.87	0.00	104.57	0.00	110.33	0.00
B18	6.8	39.11	4.3	96.98	0.16	104.69	0.17	110.45	0.18
B19	6.9	37.60	3.7	83.56	8.41	90.20	9.07	95.17	9.57

4 ANALYSIS METHODS

4.1 UNDRAINED SHEAR STRENGTH

The interpreted undrained shear strength s_{u0} was obtained by linearly fitting the measured cone resistance divided by the cone factor within a given clay unit. Only positive gradients were considered, so that when a negative slope was derived, s_{u0} was taken as the average value along a given clay layer.
When using the method of Hanna & Meyerhof (1980) and the load spread method (ISO 19905-1, 2016), the undrained shear strength s_{u0} was averaged over a depth of $B/2$, or, should that exceed it, over the remaining layer thickness. For the method of Hu et al. (2014), however, the undrained shear strength was not averaged, as it explicitly accounts for a positive gradient ρ.

4.2 BEARING CAPACITY IN CLAY LAYERS

The formula provided by ISO 19905-1 (2016) was applied to calculate the bearing capacity in clays:

$$Q_V = A(s_u N_c s_c d_c + p'_0)$$

where s_u is the averaged undrained shear strength, as explained in 4.1.

4.3 HANNA AND MEYERHOF

The method of Hanna & Meyerhof (1980) was applied as reported in ISO 19905-1 (2016):

$$Q_V = Q_{u,b} - AH\gamma'_s + 2AH(H\gamma'_s + 2p'_0)K_s \tan\left(\frac{\varphi'}{B}\right)$$

where $Q_{u,b}$ is the bearing capacity of the underlying clay at the sand-clay interface, as calculated in 4.2. The overburden pressure p_0' was considered at spudcan depth, as depicted in ISO 19905-1 (2016). The punching shear factor K_s was taken from the chart shown in ISO 19905-1 (2016), by choosing the line closest to the value of φ'.

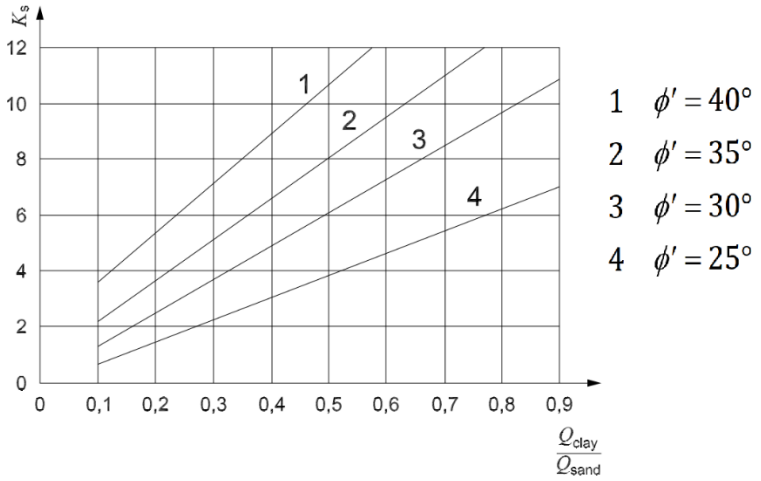

Figure 2: Bearing capacity ratio versus coefficient of punching shear (ISO 19905-1, 2016).

The value of Q_{clay} corresponds to $Q_{u,b}$, while the value of Q_{sand} was taken as the bearing capacity of sand as determined in ISO 19905-1 (2016):

$$Q_{\text{sand}} = A\left(\gamma' d_\gamma N_\gamma \pi \frac{B}{2} + p_0' d_q N_q \pi\right)$$

where the bearing capacity factors N_γ, d_γ, N_q and d_q were determined according to ISO 19905-1 (2016). The overburden pressure p_0' was taken at the spudcan depth, thus yielding a different K_s at every penetration increment.
A lower bound value K_s was considered by adapting the approximation proposed by The Society of Naval Architects and Marine Engineers (2008):

$$K_s \approx \frac{3s_u}{B\gamma_s'}$$

when the ratio Q_{clay}/Q_{sand} is lower than 0.1.

4.4 LOAD SPREAD METHOD

The load spread method was applied according to ISO 19905-1 (2016), where a fictitious footing is derived as follows:

$$B' = B + 2\frac{H}{n_s}$$

The fictious footing was then used in the formula shown in 4.2 to derive $Q_{u,b}$, by recalculating the spudcan bearing area with the fictitious footing, where s_u is the averaged undrained shear strength at the sand-clay interface and overburden pressure p_0' is taken at the spudcan depth. The bearing capacity in the sand layer is finally defined as

$$Q_V = Q_{u,b} - W$$

where

$$W = 0.25\pi\left(B + 2\frac{H}{n_s}\right)^2 H\gamma_s{}'$$

is the weight of the sand between the spudcan and the sand-clay interface.

The load-spread factor n_s determines the width increment of B' with respect to B, where a larger values indicates a smaller spread. Values ranging from 3 to 5 are used in standard practice (ISO 19905-1, 2016), and the two boundary values were used in this paper.

4.5 HU ET AL. METHOD

The method proposed by Hu et al. (2014) assumes that the peak resistance is reached at a depth of 12% of the sand layer thicknes (H_s):

$$Q_{\text{peak}} = A(N_{c0} + q_0 + 0.12\gamma_s' H_s)\left[1 + \frac{1.76H_s}{B}\tan(\psi)\right]^{E^*} + A \cdot \frac{\gamma_s'}{2\tan(\psi)(E^*+1)}\left\{1 - \left[1 - \frac{1.76H_s}{B}\tan(\psi)\right]\left[1 + \frac{1.76H_s}{B}\tan(\psi)\right]^{E^*}\right\}$$

with

$$E^* = 2\left\{1 + D_F\left[\frac{\tan(\varphi^*)}{\tan(\psi)} - 1\right]\right\},$$

$$\tan(\varphi^*) = \frac{\sin(\varphi')\cos(\psi)}{1 - \sin(\varphi')\sin(\psi)}$$

and

$$N_{c0} = 6.34 + 0.56\frac{\rho[B + 1.76H_s\tan(\psi)]}{s_{um}}.$$

The formula for N_{c0} is provided by Hu et al. (2015) and was derived from Houlsby & Martin (2003).
The D_F was defined for flat and conical footings (Hu, Stanier, Wang, & Cassidy, 2015):

$$D_F = 0.642\left(\frac{H_s}{B}\right)^{-0.576} \quad \text{as} \quad 0.16 \le \frac{H_s}{B} \le 1 \quad \text{(conical footings)}$$

and

$$D_F = 0.623\left(\frac{H_s}{B}\right)^{-0.174} \quad \text{as} \quad 0.21 \le \frac{H_s}{B} \le 1.12 \quad \text{(flat footings).}$$

The bearing capacity in the clay layer is calculated considering the influence of the sand plug (Hu, Wang, Cassidy, & Stanier, 2014):

$$Q_{\text{clay}} = A(N_c s_{u0} + 0.9H_s\gamma_c') \quad \text{as} \quad 0.16 \le \frac{H_s}{B} \le 1.00$$

where (Hu & Cassidy, 2017)

$$N_c = \left(9 + 0.9\frac{\rho B}{s_{um}}\right) + \left(10 + \frac{\rho B}{s_{um}}\right)\frac{H_s}{B} \quad \text{for} \quad 0 \le \frac{\rho B}{s_{um}} \le 3$$

The bearing capacity in the sand layer between $0.12H_s$ and the sand-clay interface is obtained by means of linear interpolation between Q_{peak} and Q_{clay} at the layers interface.
The dilation angle ψ was calculated as (Hu, Stanier, Cassidy, & Wang, 2014):

$$\psi = \frac{\varphi' - \varphi_{cv}'}{0.8}$$

The critical state friction angle φ_{cv}' was assumed to be equal to φ'. Kort et al. (2013) have also used values of φ_{cv}' in similar range, from 34° to 40.4°, for a North Sea sand.
Locations where the ratio $\frac{H_s}{B}$ was lower than 0.16 were not analysed with the Hu method, namely A1 (all vessels), A2 (all vessels), A8 (all vessels) and B15 (V1).

4.6 STRUCTURAL SPUDCAN REACTION AND BACKFILL

According to ISO 19905-1 (2016), the available structural spudcan reaction is

$$V_L = Q_V - W_{BF} + B_S$$

where W_{BF} is the weight of backfill and B_S is the soil buoyancy of the spudcan below the maximum bearing area. For simplicity, the backfill weight was calculated as (ISO 19905-1, 2016)

$$W_{BF} = \max\{\gamma'[A \cdot D - (V_{\text{spud}} - V_D)], 0\}$$

and the soil buoyancy B_S was neglected.
The leg penetration is then computed as the minimum depth at which available structural spudcan reaction is equal or exceeds the exerted load from the vessel.

5 RESULTS AND DISCUSSION

The soil profiles presented in Section 3.3 were each analysed, when all boundary conditions were met, with the methods presented across Section 4. Three V_L curves (LB, BE and UB), one for each of the selected N_{kt} values, were obtained. Punch-through was predicted whenever the final leg penetration exceeded the thickness of the top sand layer. The reported penetrations were not corrected in a second step by the presence of a sand plug, as the current study focusses only on the prediction of the peak punch through load. The methods are evaluated in Table 4 on their performance on 3 criteria: if punch-through (or lack thereof) can be correctly predicted, if it can be predicted when it did not occur (false positive), or if the location can be predicted as risk-free, when in fact it did occur (false negative). Table 5 summarises the performance of each method.

Table 5: Method performance summary.

Method	Vessel	Correct prediction			False positive			False negative		
		LB	BE	UB	LB	BE	UB	LB	BE	UB
Hanna & Meyerhof	V1	28	28	27	-	-	-	1	1	2
	V2	8	8	8	-	-	-	2	2	2
	V3	10	10	10	-	-	-	-	-	-
Load-spread, $n_s = 5$	V1	27	28	27	1	-	-	1	1	2
	V2	8	8	8	-	-	-	2	2	2
	V3	10	10	10	-	-	-	-	-	-
Load-spread, $n_s = 3$	V1	27	26	24	-	-	-	2	3	5
	V2	8	8	8	-	-	-	2	2	2
	V3	10	10	10	-	-	-	-	-	-
Hu (flat footing)	V1	20	20	20	-	-	-	5	5	5
	V2	8	8	8	-	-	-	2	2	2
	V3	10	10	10	-	-	-	-	-	-
Hu (conical footing)	V1	20	20	20	-	-	-	5	5	5
	V2	8	8	8	-	-	-	2	2	2
	V3	10	10	10	-	-	-	-	-	-

Only one false positive result was observed, obtained by the load-spread method with $n_s = 5$. The Hanna & Meyerhof and the load-spread method with $n_s = 5$ registered ten false negatives, while 16 were recorded by the load-spread method with $n_s = 3$. The Hu et al. method did not predict any of the punch-through cases that occurred. Overall, Figure 3 to Figure 5 show how the Hanna & Meyerhof method and the load-spread method with $n_s = 5$ correctly predicted within their results envelope the failure behaviour at all locations for all three vessels, except for vessel V2 at A1, which indeed yielded a much higher N_{kt} when fitting the penetration records, and for both vessels V1 and V2 at A4. The load-spread method with $n_s = 3$, on top of V2 at A1, and vessels V1 and V2 at A4, could not predict a punch-through within its result envelope also for vessel V1 at B15. It should also be noted that the considered range for N_{kt} is narrow (23.3 – 26.5), while in practice the difference between the LB and UB of N_{kt} can be 10 or more.

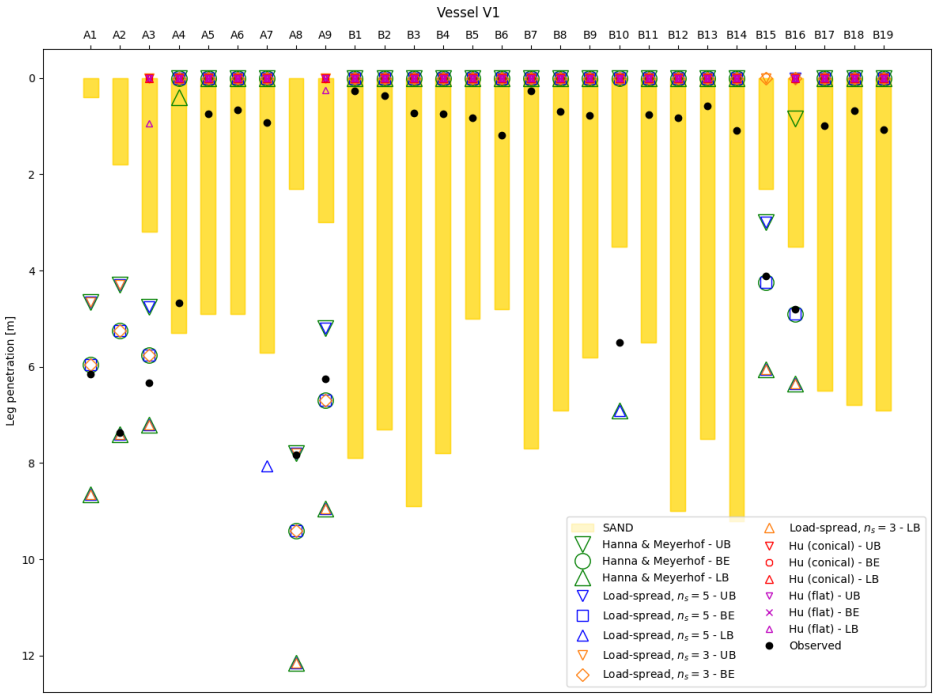

Figure 3: Overview of the leg penetration results for Vessel 1.

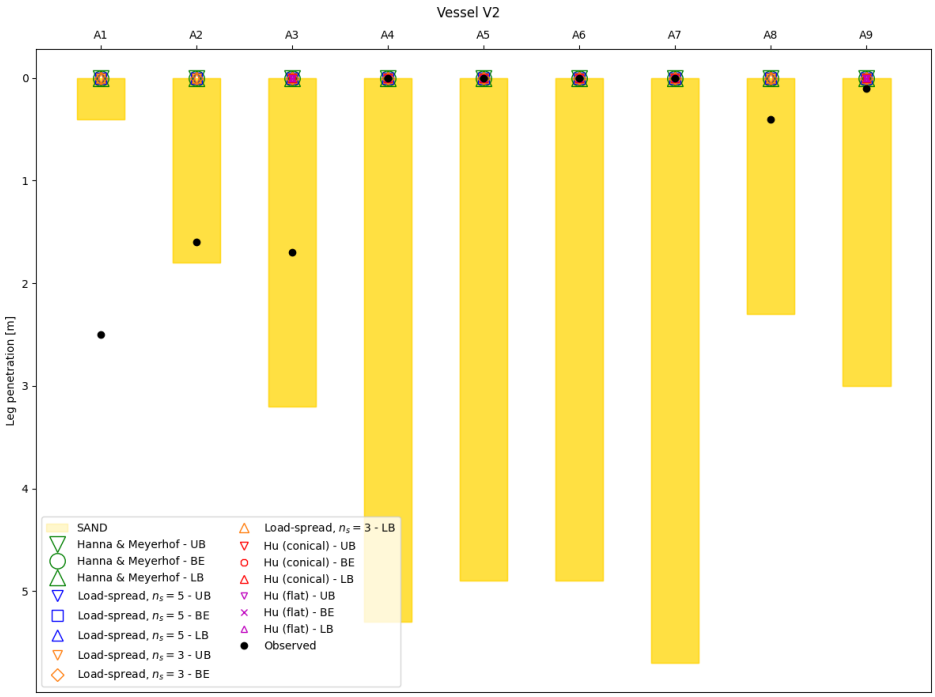

Figure 4: Overview of the leg penetration results for Vessel 2.

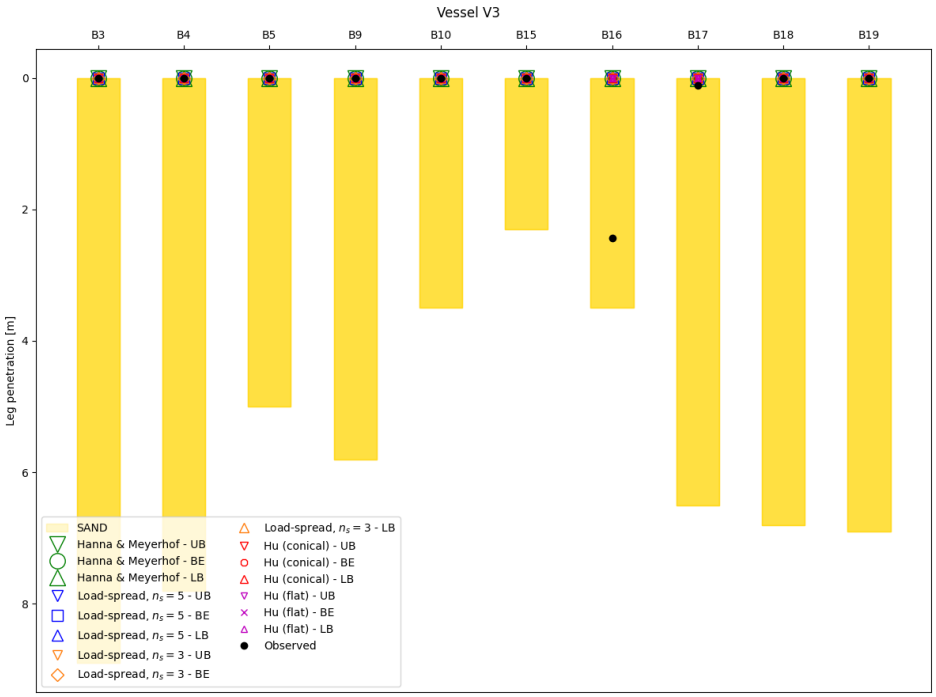

Figure 5: Overview of the leg penetration results for Vessel 3.

Since it was not possible to correctly predict punch-throughs with the Hu method, the fitting exercise done in Section 3.2 was then repeated, but by considering the Hu method (for flat footings). Only the cases of vessel V1 at locations A3, A9, B10 and B16 were considered, since they were the only ones where the recorded penetration reached the clay layer and where the ratio $\frac{H_s}{B}$ was larger than 0.16. The resulting N_{kt} ranged from 35.25 to 40.27, well above the values indicated in Section 3.2.

6 CONCLUSIONS

Three different methods to estimate the bearing capacity of sand overlying a clay layer were compared for Belgian windfarm sites. Locations with a relatively constant, well-documented stratigraphy were chosen to maximise confidence on the results. Only the recordings of the leg closest to the cpt (approx 30m-40m distance) was considered.

For two of these three methods, two alternatives were analysed, thus yielding five different sets of results. Three different vessels were considered. Overall, the method from Hanna & Meyerhof and the load-spread method have shown good agreement with the results, despite a narrow range of N_{kt} values. The method from Hanna & Meyerhof has shown the best performance, by correctly predicting most scenarios and with only two locations, when considering V1 and V2, where it failed to predict a punch-through (false negative) in all conditions. The load-spread method with $n_s = 5$ performed almost equally as well, with the only difference of predicting in lower bound conditions a punch-through when in fact it did not occur (false positive). The load-spread method with $n_s = 3$ also registered a false positive in all conditions at the same locations as the two previous methods, but also registered a false negative at one location visited by Vessel 1 in both best estimate and upper bound conditions, and two more in upper bound conditions. The two variants of the Hu method correctly predicted when punch-through did not occur but reported a false positive at four other locations (where the method is applicable). An exercise on the sensitivity of N_{kt} using the Hu method was performed. A fit would be obtained on locations A3, A9, B10 and B16 for vessel V1 by increasing N_{kt} to values ranging between 35.25 to 40.27, which is considered excessive compared to reported values from laboratory tests.

Further studies on this dataset (and others) are recommended, e.g. to quantify the sensitivity of the calculations to the thickness of the overlying sand layer, especially for locations with a low ratio $\frac{H_s}{B}$, to the precision of the recorded penetrations, to the N_{kt} values by fitting them considering punch-through, and to the spudcan shape.

REFERENCES

Hanna, A. M., & Meyerhof, G. G. (1980). Design charts for ultimate bearing capacity of foundations on sand overlying soft clay. *Canadian Geotechnical Journal, 17(2)*, 300-303.

Houlsby, G. T., & Martin, C. M. (2003). Undrained bearing capacity factors for conical footings on clay. *Géotechnique, 53(5)*, 513-520.

Hu, P. (2015). Predicting punch-through failure of a spudcan on sand overlying clay. *Doctoral dissertation*. Perth: University of Western Australia.

Hu, P. S., S. A., W. D., & Cassidy, M. J. (2015). A comparison of full profile prediction methods for a spudcan penetrating sand overlying clay. *Géotechnique Letters, 5(3)*, 131-139.

Hu, P., & Cassidy, M. J. (2017). Predicting jack-up spudcan installation in sand overlying stiff clay. *Ocean Engineering, 146*, 246-256.

Hu, P., Stanier, S. A., Cassidy, M. J., & Wang, D. (2014). Predicting peak resistance of spudcan penetrating sand overlying clay. *Journal of Geotechnical and Geoenvironmental Engineering, 140(2)*.

Hu, P., Stanier, S. A., Wang, D., & Cassidy, M. J. (2015). Effect of footing shape on penetration in sand overlying clay. *International Journal of Physical Modelling in Geotechnics, 16(3)*, 119-133.

Hu, P., Wang, D., Cassidy, M. J., & Stanier, S. A. (2014). Predicting the resistance profile of a spudcan penetrating sand overlying clay. *Canadian Geotechnical Journal, 51(10)*, 1151-1164.

ISO 19905-1. (2016). *Petroleum and natural gas industries — Site-specific assessment of mobile offshore units — Part 1: Jack-ups.* Vernier, Geneva, Switzerland: International Organization for Standardization.

Jamiolkowski, M., Lo Presti, D. C., & Manassero, M. (2003). Evaluation of relative density and shear strength of sands from CPT and DMT. *Soil behavior and soft ground construction*, 201-238.

Kort, D., Raymackers, S., Hofstede, H., & Meyer, V. (2013). Leg penetration assessments for self-elevating tubular leg units in sand over clay conditions. In M. Hicks, J. Dijkstra, M. Lloret-Cabot, & M. Karstunen, *Installation Effects in Geotechnical Engineering* (pp. 184-191). London: Taylor & Francis Group.

Le Bot, S., Van Lancker, V., Deleu, S., De Batist, M., & Henriet, J. (2003). *Tertiary and quaternary geology of the Belgian Continental Shelf.* Brussels: PPS Science policy .

Schmertmann, J. (1978). *Guidelines for cone penetration test: performance and design.* Washington D.C., United States: Federal Highway Administration.

SNAME. (2008). Techincal and Research Bulletin 5-5A. *Guidelines of Site Specific Assessment of Mobile Jack-Up Units*.

Sonnema, W., Brinkman, S., Brinkgreve, R. B., & Pisanò, F. (2023). Preloading of four-legged jack-ups in clay: Geotechnical time effects and. (Elsevier, Ed.) *Ocean Engineering, 278*.

Versteele, H., Cathie, D. N., Kuo, M. Y., & Raymackers, S. (2017). Planning the preloading procedure to account for rate-effects in clays. *International Conference: The Jack-Up* . City: University of London.

APPENDIX

Table 6: Notation.

A	Spudcan maximum bearing area [m^2]
B	Spudcan maximum bearing diameter [m]
B_S	Soil buoyancy of the spudcan below the maximum bearing area [kN]
d_c, d_q, d_γ	Bearing capacity depth factor [-]
D_F	Distribution factor
E^*	Algebraic parameter
H	Thickness of sand layer between spudcan maximum bearing area and sand-clay interface [m]
H_s	Total thickness of sand layer overlying clay [m]
I_c	Soil Behavior Type Index [-]
K_s	Punching-shear factor
N_c, N_q, N_γ	Bearing capacity factor [-]
N_{c0}	Bearing capacity factor of a clay at base level of a circular foundation [-]
N_{kt}	Cone factor [-]
n_s	Load-spread factor [-]
p_0'	Overburden pressure at the depth of the spudcan maximum bearing area [kPa]
q_0	Overburden pressure on top of sand layer[kPa]
Q_{clay}	Gross ultimate bearing capacity in a caly layer penetrated by a sand plug [kN]
Q_{peak}	Peak gross ultimate bearing capacity in sand layer susceptible to punch-throguh [kN]
Q_{sand}	Gross ultimate bearing capacity in a sand layer without interactions [kN]
Q_V	Gross ultimate bearing capacity [kN]
$Q_{u,b}$	Gross ultimate bearing capacity of underlying clay layer at sand-clay interface [kN]
s_c, s_q, s_γ	Bearing capacity shape factor [-]
s_u	Undrained shear strength averaged over half spudcan diameter [kPa]
s_{u0}	Interpreted undrained shear strength [kPa]
s_{um}	Interpreted undrained shear strength at the sand-clay interface [kPa]
V_D	Volume of the spudcan below the maximum bearing area [m^3]
V_L	Available structural spudcan reaction [kN]
V_{spud}	Spudcan volume [m^3]
W	Weight of sand between the spudcan maximum bearing area and the sand clay interface [kN]
W_{BF}	Backfill weight [kN]
γ_c'	Submerged unit weight of clay [kN/m^3]
γ_s'	Submerged unit weight of sand [kN/m^3]
ρ	Shear strength gradient [kPa/m]
φ'	Effective friction angle [°]
φ_{cv}'	Critical state effective friction angle [°]
φ^*	Reduced friction angle due to non-associated flow rule [°]
ψ	Dilation angle [°]